Research Paper

Ordovician horseshoe crab body and trace fossil association preserved in a unique taphonomic setting

Russell D.C. Bicknell [a,b,c,*] , Julien Kimmig [d,e] , Carmela Cuomo [f,g] , Aaron Goodman [h,i,j] ,
Gregory D. Edgecombe [k] , Benoit Issautier [l] , Yannick Callec [l] , Jan Freedman [m]

[a] College of Science and Engineering, Flinders University, GPO 2100, Adelaide, SA 5001, Australia
[b] Division of Paleontology (Invertebrates), American Museum of Natural History, New York, NY 10024, USA
[c] Palaeoscience Research Centre, School of Environmental & Rural Science, University of New England, Armidale, NSW 2351, Australia
[d] Paläontologie und Evolutionsforschung, Abteilung Geowissenschaften, Staatliches Museum für Naturkunde Karlsruhe, Karlsruhe 76133, Germany
[e] The Harold Hamm School of Geology & Geological Engineering, University of North Dakota, Grand Forks, ND 58202, USA
[f] Invertebrate Paleontology Division, Yale Peabody Museum, New Haven, CT 06520, USA
[g] Limulus Ranch LLC, Hamden, CT 06514, USA
[h] Department of Entomology, University of Illinois Urbana Champaign, Urbana, Il 61801, USA
[i] Division of Invertebrate Zoology, American Museum of Natural History, New York, NY 10024, USA
[j] City University of New York, Graduate Center, New York, NY 10016, USA
[k] The Natural History Museum, Cromwell Road, London SW7 5BD, UK
[l] BRGM, 3 Av. Claude Guillemin, 45060 Orleans Cedex, France
[m] The Royal Commission for AlUla, 7747 Amr AlDamari Street, Riyadh, Kingdom of Saudi Arabia

ARTICLE INFO

ABSTRACT

Horseshoe crabs (Xiphosura) have a deep fossil record but are exceedingly rare within early Palaeozoic deposits. Here, we report a new xiphosuran from the Middle Ordovician (Darriwilian) of AlUla, Saudi Arabia—one of the oldest documented horseshoe crabs that also exhibits strikingly large size for the age. The specimens, preserved in multiple lower shoreface and storm-deposited layers, include three-dimensionally preserved prosomae and detailed impressions, all associated with trace fossils assigned to the new ichnospecies, *Selenichnites sursum-deorsum*. All fossils are preserved dorsal-down—a unique taphonomic mode for xiphosurans—interpreted as storm-mediated transport of individuals followed by unsuccessful escape attempts. The recurrence of these horseshoe crab fossils across multiple stratigraphic surfaces suggests occupation of the same region over the timespan of cyclical storms, analogous to spawning behaviours in modern horseshoe crabs. Palaeoclimatic re-constructions of AlUla in the Middle Ordovician place the new horseshoe crabs within a seasonally variable nearshore environment, reflecting the ecological conditions of modern xiphosurans. These findings evidence the oldest association of horseshoe crab body and trace fossils (mortichnia), and hint at an Ordovician origin of behaviours observed in extant Xiphosura.

1. Introduction

The Great Ordovician Biodiversification Event (GOBE) is considered a vital evolutionary radiation that occurred ~470–460 mya (Servais and Harper, 2018). It records an unprecedented increase in marine biodiversity across all phyla during this time period (Servais et al., 2010; Harper et al., 2015). A combination of environmental and ecological factors—increased oxygen levels, changing ocean chemistry, and shifts in predation pressures—drove the radiation (Servais et al., 2010;

Edwards, 2019). Facets of modern marine ecosystems were established, significantly shaping the evolutionary trajectory of marine life (Webby et al., 2004; Servais et al., 2010; Harper et al., 2015; Servais and Harper, 2018; Edwards, 2019).

The GOBE saw the origin of animal groups that are seen in modern biotas. Among these, the horseshoe crabs (Xiphosura)—the only modern marine euchelicerates (Størmer, 1952; Shuster, 1982; Shuster, 2001)—had an Ordovician origin (Rudkin and Young, 2009; Lamsdell et al., 2023). Horseshoe crabs have a fossil record spanning over ~480 million

---

years, during which time they experienced two major morphological and taxonomic radiations—the Carboniferous and Triassic (Bicknell and Pates, 2020; Lamsdell, 2020; Bicknell et al., 2022). Presently, the oldest known horseshoe crabs are considered un-described specimens from the Lower Ordovician (Tremadocian) of western Utah and southeastern Idaho (Adrain et al., 2023) and the Lower Ordovician (Floian) Fezouata Lagerstätte, Morocco (Van Roy et al., 2015; Lamsdell and Ocon, 2025), as well as named younger species from the Upper Ordovician (Sandbian-Katian) of Canada (Rudkin and Young, 2009; Lamsdell et al., 2023) and the USA (Lamsdell et al., 2025). A Silurian (Ludlow) species from the USA has also recently been documented (Lamsdell, 2025). These early xiphosurans have ovate, shovel, to crescentic prosomae and a fused thoracetron expressing tergites—structures ancestral to the extant morphotype. Here we document new, large Middle Ordovician horseshoe crab body fossils associated with trace fossils from the Darriwilian of Saudi Arabia that shed light on behaviour in early Xiphosura.

2. Geological context

AlUla, in northwest Saudi Arabia, is a geologically diverse region. It is a part of the Arabian Shield, which includes Precambrian igneous and metamorphic rocks, as well as Cambrian and Early Ordovician sandstones (Hadly, 1987). Extensive lava fields developed from around 10 mya until 500,000 years ago due to the Red Sea rifting (Hadly, 1987; Rasul et al., 2015; Altherr et al., 2019). More recent alluvial deposits can be found across the region, especially in valleys (wadis), ranging from large water-travelled boulders to fine-grained wind-blown sand (Al-Bassam et al., 2014). Early Palaeozoic fine-grained to medium-grained quartz sandstones and conglomerates (the older Siq Sandstone and younger Quweira Sandstone and Saq Formation) dominate the central and northern part of AlUla (Hadly, 1987). The palaeogeography and fauna/ichnology of the Palaeozoic deposits of AlUla are poorly known, with only *Cruziana* and *Skolithos* trace fossils documented in the Saq Formation (Helal, 1964, 1968; Hadly, 1987).

The location of the new material consists of the Late Cambrian Quweria Sandstone and the Lower to Middle Ordovician Saq Formation. The Quweira Sandstone (= the Ram and Umm Sahm sandstones in Jordan, Quennell, 1951) reflects fluvial dominated to tidal deltaic environments, with no body or trace fossils. Conglomerates are present in the middle Quweira Sandstone in palaeo-valleys, indicating a significant sea-level drop. The Risha Member is the first unit of the Saq Formation, conformably overlying the Quweira Sandstone (El-Khayal and Romano, 1988). The Risha Member consists of poorly- to well-sorted, crossbedded sandstone typical of braided-river systems. The upper Risha Member consists of storm-dominated marine deposits containing *Cruziana* indicative of more distal marine palaeoenvironments. The transition from Risha Member to the overlying Sajir Member is a 1 m-thick, fine-grained section reflecting a shift from shoreface to proximal offshore deposits. The lower Sajir Member records repeated transgressive parasequences shifting between tidally to fluvial-influenced mouth-bar deltaic and storm-dominated deposits. The transgressions are marked by hardground and condensed levels, while marine beds are indicated by wave ripples, interference ripples, gutter casts, hummocky and swaley cross-stratification, and tidal bundles.

Distinct bedding surfaces within the middle units of the Sajir Member preserve horseshoe crab material (Fig. 1). These surfaces also record bioturbation, evidence of low sediment supply, and extensive time periods in these conditions. These condensed horizons are always overlain by repeated storm-influenced beds. The specimens considered here are all preserved upside down in lower shoreface sandstones overlain by storm dominated layers that indicate repeated, cyclical storm events. Several thin, dark red, iron- and mica-rich sandstone beds that vary between 5–50 mm in thickness preserve both *Cruziana* and Xiphosura specimens. Thicker (130–160 mm), light grey, sandstone beds that are stratigraphically above the iron rich beds preserve multiple Xiphosura body and associated trace fossils. Gutter casts, wave ripples and hummocky crossbedding indicate storm deposits. These thicker beds are overlain by thinner (10–30 mm) grey sandstone beds, interbedded with thicker (100 mm) beds.

A lack of biostratigraphic markers has precluded the determination of an absolute age for the Sajir Member. However, the Hanadir Member of the Qasim Formation that overlies the Sajir Member has been dated. Shales of the Hanadir Member are graptolite-rich (McClure, 1978) and preserve several trilobite and cryptospore species indicative of an upper Middle Ordovician (Darriwilian) age (El-Khayal and Romano, 1985; Strother et al., 2015). Trace fossils in the upper Saq Formation suggest a Lower to Middle Ordovician age (El-Khayal and Romano, 1988). As the Saq Formation underlies the Hanadir Member, we propose a Middle Ordovician, Darriwilian age, following Le Hérissé et al. (2017). Note that due to the limited biostratigraphic data, the Sajir Member may be older than this and we have used conservative (young) age estimates herein.

3. Methodology

Imaging and measurement—Specimens were imaged under LED light with an Olympus E-M1MarkIII camera. Originally, specimens were coated with ammonium chloride sublimate prior to photography to enhance contrast. However, due to the three-dimensional nature of the specimens, we present them uncoated. Measurements of specimens were gathered using digital callipers (Table 1). Specimens are housed within the Royal Commission of AlUla collections (RCU), Saudi Arabia.

Systematics of body fossils—We follow the systematic taxonomy of Rudkin et al. (2008), Lamsdell (2020), and Bicknell et al. (2024) and anatomical terms from Bicknell and Pates (2020) and Lamsdell et al. (2023) when describing the body fossils.
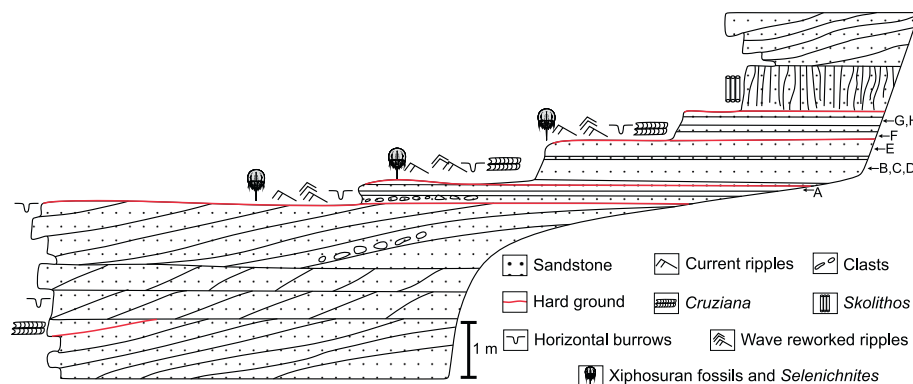

Fig. 1. Stratigraphic section of studied region showing localities of horseshoe crab fossils and traces. (A): RCU.2025.319. (B): RCU.2025.314. (C): RCU.2025.316. (D): RCU.2025.318. (E): RCU.2025.313. (F): RCU.2025.312. (G): RCU.2025.315. (H): RCU.2025.317.

Table 1
Summary of measurements for examined body and trace fossils.

Specimen	Prosomal length (mm)	Prosomal width (mm)	Trace length (mm)	Trace width (mm)	Impression length (mm)	Impression width (mm)
RCU.2025.312	47.9	84.9	20.0	38.4	–	–
RCU.2025.315	39.9	77.8	24.9	46.9	–	–
RCU.2025.313	–	–	25.8	47.3	24.6	72.3
RCU.2025.314	–	–	21.6	38.1	51.9	75.7
RCU.2025.318a	–	–	–	–	34.4	75.3
RCU.2025.318b	–	–	–	–	49.9	70.1
RCU.2025.317	–	–	27.3	45.7	34.0	71.0
RCU.2025.316	–	–	28.0	47.3	23.1	64.8
RCU.2025.319	–	–	28.6	62.3	–	13.5

Systematics of trace fossils—We follow the systematic taxonomy of Romano and Whyte, (1987; 1990; 2015) and Leibach et al. (2021) when describing the trace fossils.

Size data—To compare the size of Sajir specimens to other horseshoe crab species, we used the prosomal size data collated in Bicknell et al. (2022). Prosomal length and width measurements were natural log (ln) normalized and plotted, highlighting the position of new specimens in bivariate space.

Neoichnology—To explore the origin of the trace fossils, we used living juvenile specimens of the American horseshoe crab *Limulus polyphemus* of comparable size to Sajir specimens to reproduce the traces. A sand and clay mixture was layered on a ~25° angle in a Plexiglas^{tm} aquarium (60 cm × 29 cm × 20 cm), creating a sloped "beach" that levelled out two thirds of the way across the tank. Seawater was poured into the low end to submerge the matrix and allowed to stand for 24 h. Water was then siphoned off to expose a "beach" area, leaving 3 cm of water over the lowest part of the "beach". The juvenile *L. polyphemus* was removed from a holding tank and gently placed prosoma-down into the slope substrate to model the upside-down deposition of an individual on a sandy bed. The horseshoe crab was left for five minutes to make a trace, after which they were gently removed without disturbing the underlying substrate and returned to their aquaculture tanks. Remaining water was siphoned out without disturbing the trace. After 24 h, a cast of the trace was produced by pouring DAP Plaster of Paris^{tm} into the aquarium, beginning at the lowest point until the entire slope was covered. Once fully dry, the plaster cast was removed and a series of medium to fine-ultra paintbrushes were used to clear away sediment stuck to the cast. The cast (Fig. 2H) is housed within the Yale Peabody Museum invertebrate paleontology (YPM IP) collection.

Palaeoclimatic analyses—To estimate the palaeoenvironmental conditions that were present in AlUla during the Darriwilian, palaeoclimatic analyses were conducted using Global Circulation Models (GCM). Occurrences of the new Ordovician horseshoe crab were acquired using GPS from the type locality (27°18′56.0″, N 37°56′14.2″E). Using the *rgplates* package version 0.3.2 (Kocsis et al., 2023) in R version 4.0 (R Core Development Team, 2021), the occurrence was palaeo-rotated to the Darriwilian using Scotese's PALEOMAP (Scotese, 2016) palaeo-digital elevation model. As the Darriwilian overlaps with two palaeo-digital elevation models, the occurrence was rotated to the 460 mya and 465 mya time slices. The palaeo-rotated occurrence data placed the new Ordovician horseshoe crabs approximately ~500 km inland—a complication that is associated with palaeorotation of models (particularly epicontinental sea boundaries) that can reconstruct coastal invertebrate occurrences on land instead of in the ocean (Scotese and Wright, 2018; Goodman et al., 2025). Furthermore, the coarseness of the digital elevation models (DEM) and palaeoclimatic variables may have resulted in the placement of the specimens distal from the coast as the ocean-to-land transition is represented by limited pixels (Goodman et al., 2025). As the specimens were preserved dorsal-down, given the preservational mode and evidence for storm-mediated burial, we propose the specimens were swept onto the shoreline.

We used an equal-area (Eckert IV) projection to define a 1000 km radius around the fossil site to explore climatic and bathymetric ranges of the new Ordovician horseshoe crab and possible species dispersal. This conservative buffer is appropriate for examining global ecological niche models (see discussion in Kass et al., 2021; Goodman et al., 2025) and aligns with observations of *Limulus polyphemus*, *Carcinoscorpius rotundicauda,* and *Tachypleus gigas* that disperse > 200 km from the shoreline (Botton et al., 2003; Tang et al., 2021), although dispersal capability of horseshoe crabs is also impacted by wind and ocean currents, temperature, salinity, maturity rate, and breeding ground availability (Botton et al., 1988; Botton et al., 2003; Berkson et al., 2009; Botton et al., 2010; Carmichael and Brush, 2012; Tang et al., 2021). Within the study extent, we sampled the total amount of pixels within our study extent (n = 107) and this was repeated for the 460 mya and 465 mya time slices.

Environmental layers were generated using output from the HadCML3 climate model version 4.5 (Valdes et al., 2017), with inputs from solar luminosity, and the PALEOMAP palaeogeographic atlas (Scotese, 2016; Scotese and Wright, 2018) for the Darriwilian Stage. The GCM "HadCM3LB-M2.1aD" set of simulations (*sensu* Valdes et al. 2017) was used, with a surface resolution of 3.75° longitude × 2.75° latitude (grid box size of ~420 × 220 km; at the equator, reducing to ~200 × 280 km at 45° latitude).

The Scotese simulations are similar to the Middle Ordovician (Map numbers 80 & 80.5) simulations of Valdes et al. (2021). These simulations prescribe a pCO$_2$ concentration after Foster et al. (2017). Compared to the Valdes et al. (2021) study, simulations were run for an additional 2,000 years, with modified atmospheric and ocean physics following Sagoo et al. (2013), improving polar amplification in deep-time climates. Additionally, islands are defined correctly for calculating ocean barotropic stream function.

Climate model outputs were chosen to encapsulate the abiotic restrictions of modern and fossil horseshoe crabs (Shuster et al., 2003). Variables chosen within the Darriwilian model sets were annual mixed layer depth (in meters), annual maximum (warmest) and annual minimum (coldest) sea-surface temperature within a three-month interval (in °C), monsoon seasonality index—a proxy for tropical seasonal variability—and annual mean sea-surface temperature (in °C). Although horseshoe crabs are known to spend time on the continental shelf at depths exceeding 290 m (Botton and Ropes, 1987), we did not consider depth-related climatic variables (Goodman et al., 2025) as the geology suggests shoreline conditions. Finally, we incorporated bathymetry (in meters), derived from the DEMs that underlie the Scotese GCM simulations. All variables were rotated from a 0–360 longitudinal format to −180–180 longitudinal format to avoid cutoff at the international date line.

Environmental values from each variable within the 460 mya and 465 mya Darriwilian time slices were extracted to encapsulate the climatic range of the horseshoe crabs. These occurrence and climatic data were presented using QGIS version 3.42. Boxplots of each climatic variable were also generated using *ggplot2* (Wickham et al., 2016), consisting of the extracted environmental values and the average of the two, and performed analysis of variance and Tukey's HSD tests using the *agricolae* package (de Mendiburu and de Mendiburu, 2019). Importantly, pixel size (i.e., spatial grain) impacts the interpretation of
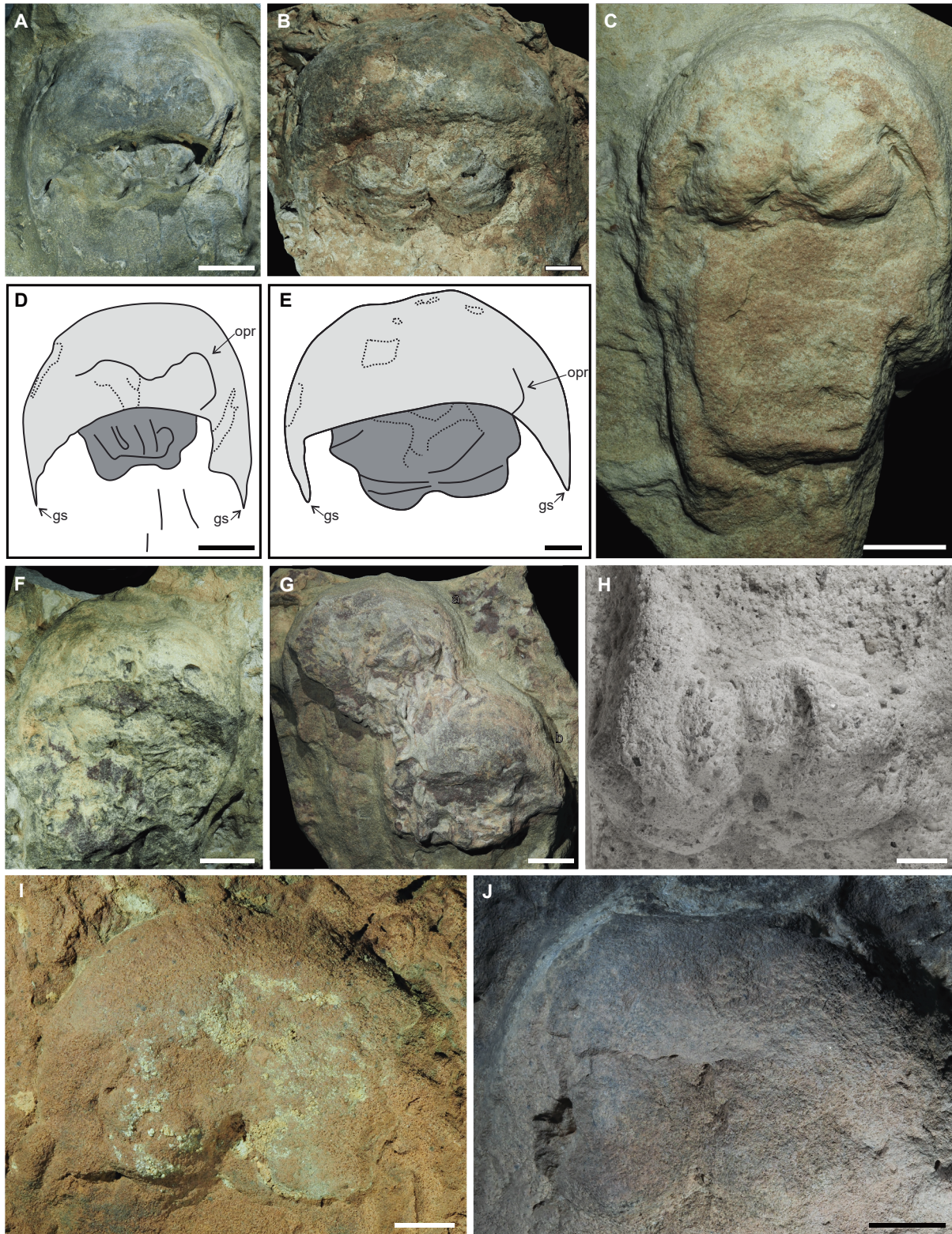
Fig. 2. Horseshoe crab body and trace fossils from AlUla, along with modern horseshoe crab traces. (A, B, D, E) Xiphosura *incertae sedis* with *Selenichnites sursumdeorsum*. (A, D) RCU.2025.312. (A) Image of specimen. (D) Line drawing of specimen. (B, E) RCU.2025.315. (B) Image of specimen. (E) Line drawing of specimen. (C, F, G) *Selenichnites sursumdeorsum* with well-defined prosomal impressions. (C) Holotype. RCU.2025.313. (F) RCU.2025.314. (G) RCU.2025.318. (a) and (b) denote different impressions on slab. (H) Impression produced by modern American horseshoe crab, *Limulus polyphemus*. YPM IP 259971. (I, J) *Selenichnites sursumdeorsum* with poorly defined prosomal impressions. (I) RCU.2025.316. (J) RCU.2025.317. RCU.2025.319 not figured. (H) image converted to greyscale. (D, E) Lighter grey: prosoma. Darker grey: *Selenichnites sursumdeorsum*. Abbreviations: gs, genal spine; opr: ophthalmic ridge. Scale bars: (A, C, D, F, G): 20 mm; (B, E, H, I, J): 10 mm. Image credit: (H): Jessica Utrup.

environmental variables, specifically bathymetry.

4. Results

Sajir specimens are preserved as three-dimensional (3D) moulds, prosoma-down (upside down) (Fig. 2). Specimens include body fossils, impressions of body fossils, and trace fossils. They are documented on several distinct bedding surfaces, cyclically deposited above each other. Bedding surfaces also show evidence of *Cruziana*, burrowing traces, and mud cracks.

The size of Sajir specimens in comparison to other xiphosurans (Fig. 3A) demonstrates that the new material is located within the largest size classes of *Mesolimulus* (Jurassic) and medium classes for *Tachypleus* (modern). These Ordovician forms were therefore substantially larger than all other Palaeozoic xiphosurans in the Bicknell et al. (2022) dataset. Additionally, the Sajir specimens are ~60 % the size of the largest known Palaeozoic xiphosuran–*Xaniopyramis linseyi*.

Comparing the cast of the *Limulus polyphemus* trace to the trace fossils
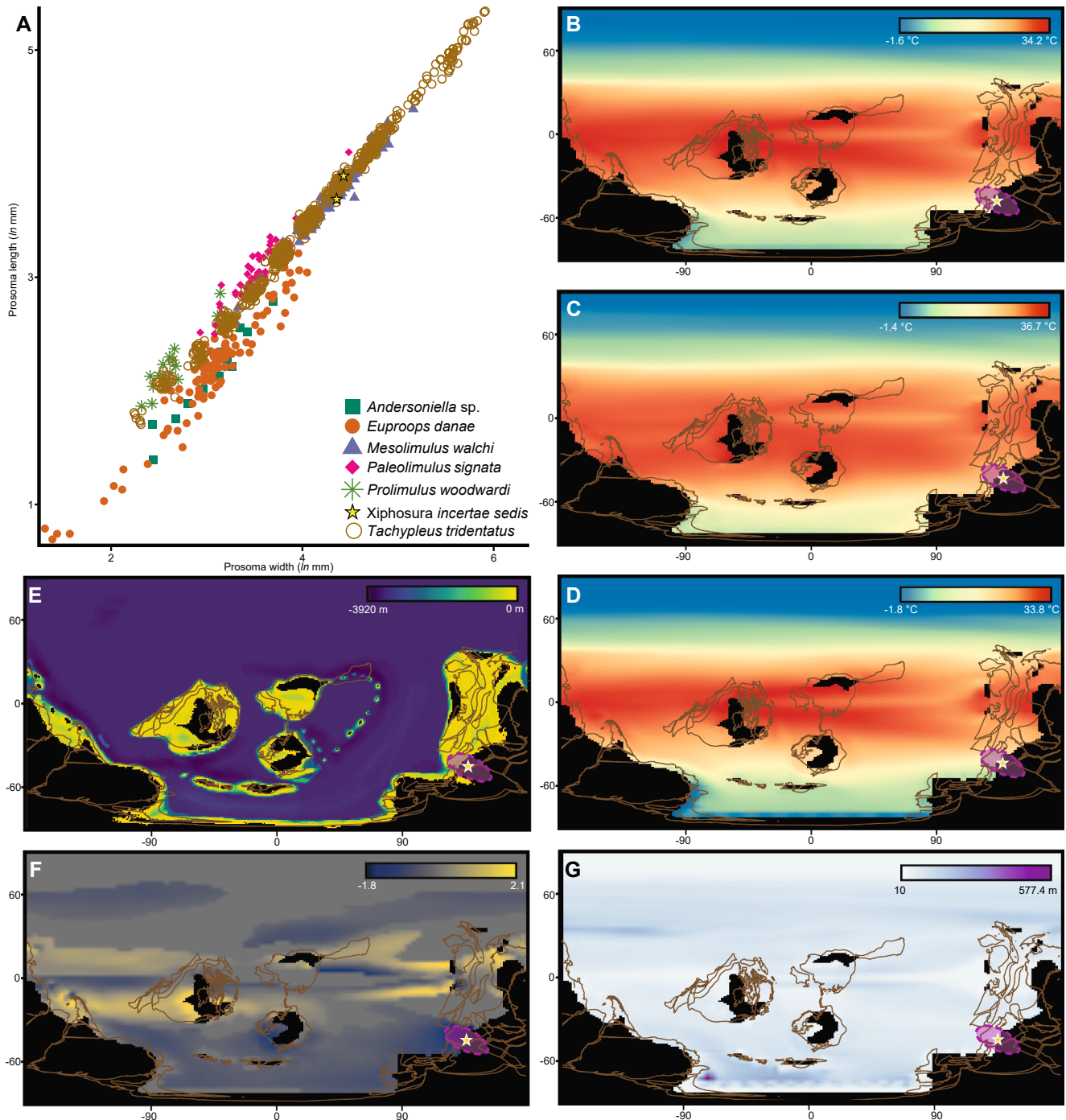

Fig. 3. Size and palaeoclimatic models associated with new xiphosuran fossils. (A) Natural log normalized size data of modern and extinct horseshoe crab prosomae showing the large size of the Saudi xiphosurans. (B–G) Palaeoclimatic models associated with the Saudi xiphosurans. Yellow star indicates type locality. Purple oval indicates 1000 km buffer. (B) Annual sea surface temperature. (C) Warmest three-month sea surface temperature. (D) Coldest three-month sea surface temperature. (E) Bathymetry. (F) Monsoon seasonality index. (G) Annual mixed layer depth. (For interpretation of the references to colour in this figure legend, the reader is referred to the web version of this article.)

considered here, marked similarities in morphology are clear (Fig. 2H). The traces record the horseshoe crab attempting to right itself on the slope and the bilobed trace morphology reflects clumping of sediment together. Motion along the prosoma-thoracetron articulation produced the clumping, recording attempts at enrolment and shifting the body to right the exoskeleton.

Palaeoclimatic models of the Ordovician present important insight into the conditions in which the Sajir specimens lived. There was an annual mean sea surface temperature range from 15.9–22.7 °C (Fig. 3B–D), a water depth range between −1,200–0 m, with most of the distribution being shallow water conditions (Fig. 3E), a monsoon seasonality index of −1.7–−1.1 (Fig. 3F), and an annual mixed layer depth range of 14–35 m (Fig. 3G).

No statistical differences in geologic stages and the average bathymetric readings, coldest season, and annual mean sea surface temperature were found (Fig. 4). Evidence was, however, found for significant differences in geologic stages and the average for Monsoon Seasonality Index ($F_{2, 346} = 7.08$, $p < 0.001$) and warmest season ($F_{2, 346} = 3.73$, $p = 0.02$) (Fig. 4). Differences in climatic variables reflect averaging across geologic stages.

Systematic palaeontology
Subphylum: Chelicerata Heymons, 1901 (Heymons, 1901)
Euchelicerata: Weygoldt and Paulus, 1979 (Weygoldt and Paulus, 1979)
Xiphosura: Latreille, 1802 (Latreille, 1802)
Xiphosura *incertae sedis*
Referred material: RCU.2025.312, RCU.2025.315
Formation, locality, and age: Sajir Member, Saq Formation, AlUla (27°18′56.0″N 37°56′14.2″E), Saudi Arabia, Middle Ordovician (Darriwilian).
Preservation: The specimens are preserved as external, 3D mould on brownish white sandstone.
Description: Isolated prosomal sections (Fig. 2) that show marked 3D relief. Prosomae measure 39.9 (RCU.2025.315) and 47.9 (RCU.2025.312) mm in length, and 77.8 (RCU.2025.315) and 84.9 (RCU.2025.312) mm in width. Prosoma crescentic, with weak, concave ophthalmic ridges on each side. Ophthalmic ridges form a rounded 'M'-shape within the posterior third of prosoma (Fig. 2D, E). Prosoma otherwise effaced. Genal spines robust, projecting posteriorly from prosoma by 25.9–35.8 mm. Posterior prosomal border curved slightly convexly anteriorly. Thoracetron and telson unknown.
Remarks: Fossil horseshoe crab species are commonly defined by characters of both prosomal and thoracetron morphologies. Examined material here is limited to two prosomae and due to this condition, we have maintained the taxon in open nomenclature; more complete specimens are needed for genus and species level assignments. However, we highlight that a distinctive 'M'-shaped ophthalmic ridge joint is observed on the prosomae. This joint shape is observed in the Devonian kasibelinurid *Patesia*, and limuloid *Bellinuroopsis*; Carboniferous belinurids (*Belinurus*, *Euproops*, *Liomesaspis*), Carboniferous and Permian *Paleolimulus*, and the Triassic *Tasmaniolimulus* (Bicknell and Pates, 2020), reinforcing the xiphosuran identity of the Saudi material, but in all cases the joint is towards the anterior third of the prosoma. The new material contrasts with these other examples in having an 'M'-shaped ophthalmic ridge joint within the posterior third of the prosoma. Compound eyes are not observed in the material. However, xiphosuran lateral compound eyes are located along ophthalmic ridges. The reduced ophthalmic ridge length in the Saudi material indicates that lateral compound eyes were located posteriorly compared to modern forms (Bicknell et al., 2019).

Systematic ichnology
Ichnogenus: *Selenichnites* Romano and Whyte, 1990 (Romano and Whyte, 1990) (= *Selenichnus* Romano and Whyte, 1987 (Romano and Whyte, 1987))
Ichnospecies: *Selenichnites sursumdeorsum*
Fig. 2.

Etymology: Named after the dorsal-down preservation, Latin for upside down.
Holotype: RCU.2025.313
Referred material: RCU.2025.312, RCU.2025.314–RCU.2025.319,
Type locality, formation, and age: Sajir Member, Saq Formation, AlUla (27°18′56.0″N 37°56′14.2″E), Saudi Arabia, Middle Ordovician (Darriwilian).
Diagnosis: Solitary crescent-shaped trace, approximately as long as wide, with inner margin of crescent interrupted in midline to give two paired lobes with long axes more or less parallel to median line. Posterior to the crescent a convex bilobate morphology with two parallel lobes, covered by transverse ridges, separated by a median line in the posterior part of the lobes, long axis of each lobe at about 30°. Trace strongly convex.
Description: Specimens are preserved as positive convex hypo-relief casts (Epichnia). Quality of preservation varies, with some specimens preserving detailed posterior bilobate-shaped morphology, whereas others preserve relatively undefined lobes.

The anterior crescent is approximately as long as wide. The prosoma is represented by bilaterally symmetrical lobes, which form thin ridges on the exterior of the trace and slope gently inwards, towards the other lobe. The crescent is interrupted in midline to give two paired lobes with long axes about the median line. The anterior margin has a slight indent in the middle, creating an M−shape. The impressions of the genal spines are nearly straight.

The posterior bilobate-shaped morphology consists of two parallel lobes that join anteriorly. They are preserved in positive convex hypo-relief and range in length between 20.0–28.0 mm and in width between 38.1–47.3 mm. There are three to four transverse corrugations at common distances of 2–5 mm. Posterior lobes terminate at the posterior end of the crescent shaped anterior.
Remarks: These trace fossils are assigned to the ichnogenus *Selenichnites*, as they preserve the rounded anterior margin and paired crescent-shaped anterolateral lobes that are typical of this ichnogenus (Romano and Whyte, 1987, 2003, 2015). The anterior morphology of the AlUla traces resembles *Selenichnites cordiformis* (Fischer, 1978), but *S. cordiformis* is missing the posterior bilobate morphology.

5. Discussion

The specimens observed here are preserved upside down without evidence for tectonically overturned beds. This is unique in the horseshoe crab fossil record. Using the depositional environment and proposed palaeoclimatic reconstructions (Fig. 3), we outline the following system as an explanation for the material. The Sajir Member represents a tidally- influenced delta where horseshoe crabs spawned proximal to the palaeo-shoreline, likely in lower shoreface conditions. During large, storm events, spawning individuals were picked up and redeposited upside down. Horseshoe crabs attempted to escape by moving along the prosoma-thoracetron articulation, producing the bilobed traces. The lack of thoracetron sections as body fossils demonstrates that posterior exoskeletal sections were damaged during failed attempts to escape. One of two taphonomic pathways then occurred—(1) the prosoma was preserved as a mould or (2) the prosoma decayed, leaving either a detailed or poorly defined impression. In the first pathway, the horseshoe crab was deposited in a localized area of anoxia (possibly from proximal algal masses), moulding the prosoma in sufficient detail in the matrix, prior to exoskeletal decay. This mould was then lithified as the body fossil. In the second pathway, the prosoma made an impression in a substrate that was too oxygen-rich. The prosoma completely decayed, preserving body fossil impressions. The extreme of this pathway is represented by specimens that show poorly defined prosomae and trace fossils. Here, either the substrate was too coarse or saturated to permit detailed impressions, or during prosomal decay sediment slumping and infilling occurred. In all pathways, the trace fossils are more consistently preserved. This taphonomic pathway was repeated multiple times,
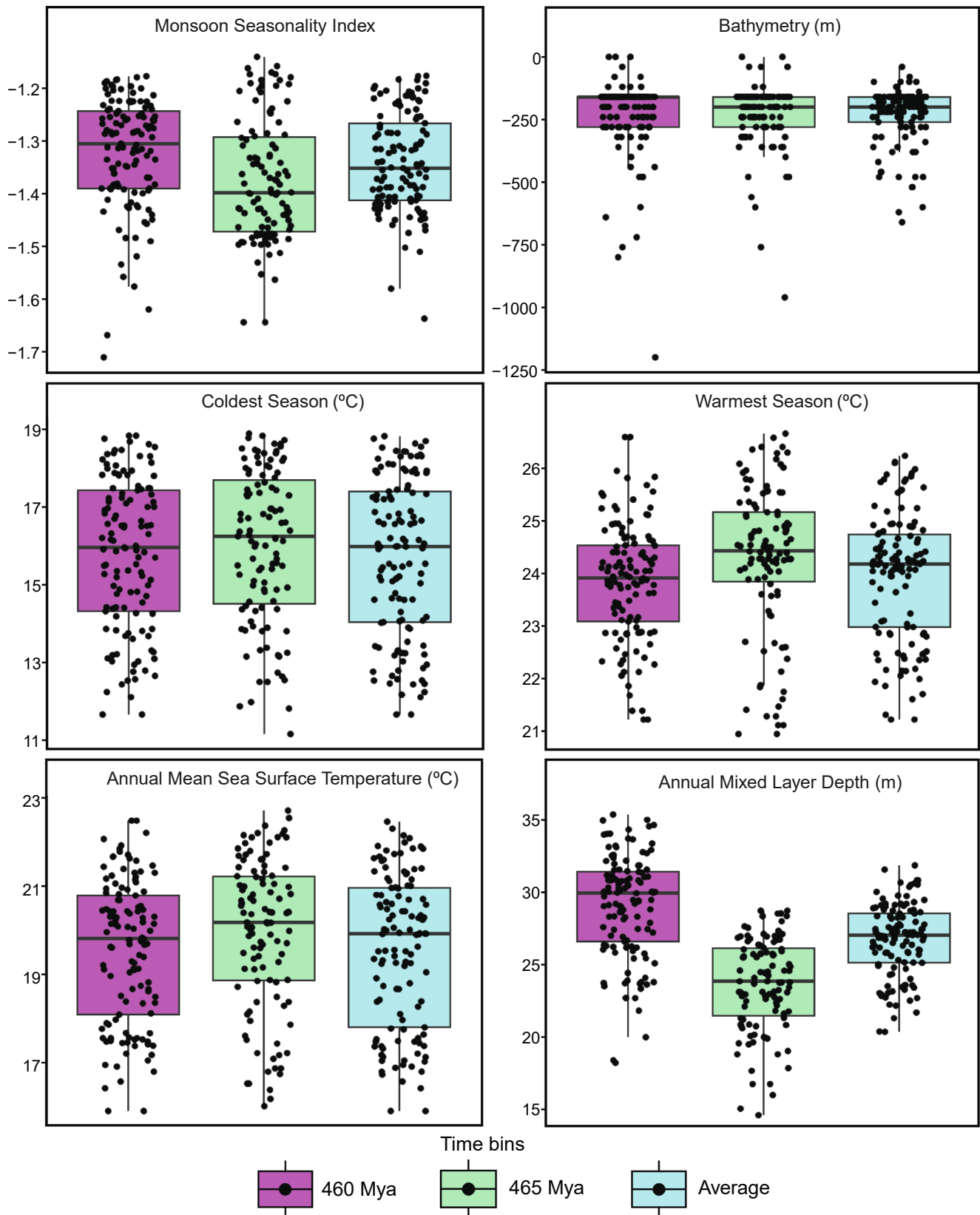
Fig. 4. Summary of comparative analyses between different time divisions of the Darriwilian.

evidenced by different bedding plains preserving xiphosuran fossils (Fig. 1).

The trace fossil posterior to the prosoma was reproduced when modern horseshoe crabs were positioned upside down on the substrate (Fig. 2H). Motion along the prosoma–thoracetron articulation reflects sediment clumping. Traces posterior to prosomae in RCU.2025.312 and RCU.2025.315 are therefore interpreted as examples of attempted escape traces, not burrowing traces. These are the oldest xiphosuran trace fossils in the marine fossil record, together with the Darriwilian *Kouphichnium* specimens from the Baykit Sandstone of Siberia (Kushlina and Dronov, 2011) and only slightly younger than the Tremadocian *Crescentichnus antarcticus* from the marginal marine sediments of the Blaiklock Glacier Group of Antarctica (Weber and Braddy, 2003; Romano and Whyte, 2015). The appearance of the similarly crescent shaped traces *Crescentichnus antarcticus* and *Selenichnites cordiformis* (the latter from the Sandbian of Colorado, USA) (Fischer, 1978) suggests that the modern prosoma shape of xiphosurans developed early in their evolution, however, both of these traces are ~50 % smaller than the examples here, suggesting that they were produced by either juveniles or a different species.

The association of the trace fossil *Selenichnites sursumdeorsum* with its trace maker is particularly important. Examples of trace fossils in association with the trace maker are extremely rare in the fossil record (Fortey and Seilacher, 1997; Fatka and Szabad, 2011; Lomax and Racay, 2012), as the trace and body fossils must both have comparable preservation potentials (Fatka and Szabad, 2011; Lomax and Racay, 2012). Horseshoe crabs have only been found in association with *Kouphichnium* tracks, where the horseshoe crab landed on the seafloor, walked for a small distance and perished (Lomax and Racay, 2012). Such traces are referred to as death traces or mortichnia. In most cases death traces are preserved in largely anoxic settings (Buatois and Mángano, 2011), which makes the herein described especially interesting, as the depositional setting does not suggest extensive anoxia. The preserved trace-makers of the studied specimens likely suffocated while they tried to escape the substrate and were buried in place.

Horseshoe crabs reaching sizes of *Mesolimulus* and *Tachypleus* in the Ordovician are unprecedented. Xiphosura of these sizes are aberrant prior to the Jurassic (Bicknell and Pates, 2020; Bicknell et al., 2022) with just two other examples—a recently documented Late Ordovician *Lunataspis* with a shovel shaped prosoma (Lamsdell et al., 2025) and a large Carboniferous paleolimulid (Siveter and Selden, 1987). The Xiphosura *incertae sedis* material considered here therefore presents strong evidence for the rise of larger horseshoe crabs within the Ordovician. Extinct horseshoe crabs clearly exceeded previous body size expectations, rivalling modern forms, much deeper within the fossil record. These large xiphosurans may have followed the pathway exhibited by trilobites or eurypterids, showing substantial increases in size in the Ordovician (Sun et al., 2025) and Siluro-Devonian (Braddy et al., 2008), respectively. This would reflect selection towards increased sizes associated with marine redox conditions (Sun et al., 2025), or size refugia (Vermeij, 2016).

Horseshoe crab body and trace fossils preserved in multiple, overlaying bedding planes illustrate that xiphosurans had occupied the same locality and environment over a timespan measured by cyclical storms. Modern horseshoe crabs return to the same spawning locality across different years (Leschen et al., 2006; Brockmann and Johnson, 2011). Genetic separation of different populations demonstrates that biologically distinct groups arise from this spawning biology (Avise et al., 1994; King et al., 2015; García-Enríquez et al., 2023). We infer that these Ordovician horseshoe crabs may have exhibited similar behaviours over deep time and highlight that this reproductive strategy is deeply rooted in the euchelicerate tree.

Palaeoclimatic modelling reinforces the origin of horseshoe crab behaviour in the Middle Ordovician. Water depth ranges are consistent with those of modern species (Botton and Ropes, 1987; Botton and Ropes, 1989). The range of annual mean sea surface temperature (15.9–22.7 °C) demonstrates a temperate environment, consistent with conditions inhabited by the American horseshoe crab (Shuster, 1982). Further, the high monsoonal seasonality Index (−1.7–−1.1) provides evidence for an environment with strong seasonal variation—consistent with modern forms (Shuster et al., 2003)—where variation in nutrient delivery (either from overturn or terrestrial runoff) results in increased primary and secondary productivity and prey consumption.

6. Conclusion

The discovery of Ordovician xiphosurans and associated attempted escape trace fossils offer a unique glimpse into early ecological strategies of Xiphosura. The inverted preservation and repeated stratigraphic recurrence of body and trace fossils evidence storm-driven burial of individuals. The shoreface context of the xiphosurans is consistent with spawning, and signals the possibility that reproductive site selectivity was established as early as the Ordovician. Together, the morphological, iconological, and palaeoenvironmental data presented herein highlight the deep origin of modern behaviours within Palaeozoic marine ecosystems.

CRediT authorship contribution statement

Russell D.C. Bicknell: Writing – review & editing, Writing – original draft, Visualization, Methodology, Investigation, Formal analysis, Data curation, Conceptualization. **Julien Kimmig:** Writing – review & editing, Writing – original draft, Supervision, Resources, Methodology, Investigation, Formal analysis, Data curation, Conceptualization. **Carmela Cuomo:** Writing – review & editing, Writing – original draft, Visualization, Supervision, Resources, Methodology, Investigation, Formal analysis, Data curation, Conceptualization. **Aaron Goodman:** Writing – review & editing, Writing – original draft, Visualization, Validation, Software, Resources, Methodology, Investigation, Formal analysis, Data curation, Conceptualization. **Gregory D. Edgecombe:** Writing – review & editing, Writing – original draft, Validation, Supervision, Investigation, Formal analysis, Conceptualization. **Benoit Issautier:** Writing – review & editing, Investigation. **Yannick Callec:** Writing – review & editing, Investigation. **Jan Freedman:** Writing – review & editing, Writing – original draft, Validation, Resources, Methodology, Investigation, Data curation, Conceptualization.

Appendix A. Supplementary material

Supplementary data to this article can be found online at https://doi.org/10.1016/j.gr.2025.11.011.

References

Adrain, J.M., Lerosey-Aubril, R., Edgecombe, G.D., 2023. The origin of horseshoe crabs: discovery of three-dimensionally preserved xiphosuran species in the lower Tremadocian (lower Ordovician) of the Great Basin, Western USA. Geol. Soc. Am. Abstr. Programs 55. https://doi.org/10.1130/abs/2023AM-394825.

Al-Bassam, A.M., Khalil, A.R., Kassem, O.M., 2014. Using updated DurovPwin program for hydro-chemical data processing: Case study of Al-Ula area, Saudi Arabia. Rec. Adv. Environ. Sci. Geos. 75–81.

Altherr, R., Mertz-Kraus, R., Volker, F., Kreuzer, H., Henjes-Kunst, F., Lange, U., 2019. Geodynamic setting of Upper Miocene to Quaternary alkaline basalts from Harrat al 'Uwayrid (NW Saudi Arabia): constraints from KAr dating, chemical and Sr-Nd-Pb isotope compositions, and petrological modeling. Lithos 330, 120–138.

Avise, J.C., Nelson, W.S., Sugita, H., 1994. A speciational history of "living fossils": molecular evolutionary patterns in horseshoe crabs. Evol. 48, 1986–2001.

Berkson, J., Chen, C.-P., Mishra, J., Shin, P., Spear, B., Zaldívar-Rae, J., 2009. A discussion of horseshoe crab management in five countries: Taiwan, India, China, United States, and Mexico. Biol. Conservat. Horseshoe Crabs 465–475.

Bicknell, R.D.C., Amati, L., Ortega Hernández, J., 2019. New insights into the evolution of lateral compound eyes in Palaeozoic horseshoe crabs. Zoo. Jour. Linn. Soc. 187, 1061–1077.

Bicknell, R.D.C., Kimmig, J., Budd, G.E., Legg, D.A., Bader, K.S., Haug, C., Kaiser, D., Laibl, L., Tashman, J.N., Campione, N.E., 2022. Habitat and developmental constraints drove 330 million years of horseshoe crab evolution. Biol. Jour. Linn. Soc. 136, 155–172.

Bicknell, R.D.C., Kimmig, J., Smith, P.M., Scherer, T., 2024. An enigmatic euchelicerate from the Mississippian (Serpukhovian) and insights into invertebrate preservation in the Bear Gulch Limestone. Montana. Amer. Mus. Nov. 2024, 1–16.

Bicknell, R.D.C., Pates, S., 2020. Pictorial atlas of fossil and extant horseshoe crabs, with focus on Xiphosurida. Frontiers Ear. Sci. 8, 98.

Botton, M.L., Loveland, R.E., Jacobsen, T.R., 1988. Beach erosion and geochemical factors: influence on spawning success of horseshoe crabs (*Limulus polyphemus*) in Delaware Bay. Mar. Biol. 99, 325–332.

Botton, M.L., Ropes, J.W., 1987. Populations of horseshoe crabs, *Limulus polyphemus*, on the northwestern Atlantic continental shelf. Fishery b. 85, 805–812.

Botton, M.L., Ropes, J.W., 1989. Feeding ecology of horseshoe crabs on the continental shelf, New Jersey to North Carolina. Bull. Mar. Sci. 45, 637–647.

Botton, M.L., Shuster Jr., C.N., Keinath, J.A., 2003. Horseshoe crabs in a food web: who eats whom?, In: Shuster Jr., C.N., Barlow, R.B., Brockmann, H.J. (Eds.), The American horseshoe crab. Harvard University Press, Cambridge, pp. 133–153.

Botton, M.L., Tankersley, R.A., Loveland, R.E., 2010. Developmental ecology of the American horseshoe crab *Limulus polyphemus*. Cur. Zool. 56, 550–562.

Braddy, S.J., Poschmann, M., Tetlie, O.E., 2008. Giant claw reveals the largest ever arthropod. Biol. Lett. 4, 106–109.

Brockmann, H.J., Johnson, S.L., 2011. A long-term study of spawning activity in a Florida Gulf Coast population of horseshoe crabs (*Limulus polyphemus*). Estuar. Coasts 34, 1049–1067.

Buatois, L.A., Mángano, M.G., 2011. Ichnology: Organism-substrate interactions in space and time. Cambridge University Press, Cambridge.

Carmichael, R.H., Brush, E., 2012. Three decades of horseshoe crab rearing: a review of conditions for captive growth and survival. Rev. Aqua. 4, 32–43.

de Mendiburu, F., de Mendiburu, M.F., 2019. Package 'agricolae'. R Package, Version 1, 1143–1149.

Edwards, C.T., 2019. Links between early Paleozoic oxygenation and the Great Ordovician Biodiversification Event (GOBE): a review. Palaeoworld 28, 37–50.

El-Khayal, A.A., Romano, M., 1985. Lower Ordovician trilobites from the Hanadir Shale of Saudi Arabia. Palaeontology 28, 401–412.

El-Khayal, A.A., Romano, M., 1988. A revision of the upper part of the Saq Formation and Hanadir Shale (lower Ordovician) of Saudi Arabia. Geol. Mag. 125, 161–174.

Fatka, O., Szabad, M., 2011. Burrowing trilobite caught in the act. Pal. Zeit. 85, 465–470.

Fischer, W.A., 1978. The habitat of the early vertebrates: trace and body fossil evidence from the Harding Formation (Middle Ordovician). Colorado. Mount. Geol. 15, 1–26.

Fortey, R.A., Seilacher, A., 1997. The trace fossil *Cruziana semiplicata* and the trilobite that made it. Lethaia 30, 105–112.

Foster, G.L., Royer, D.L., Lunt, D.J., 2017. Future climate forcing potentially without precedent in the last 420 million years. Nat. Comm. 8, 1–8.

García-Enríquez, J.M., Machkour-M Rabet, S., Rosas-Correa, C.O., Hénaut, Y., Carrillo, L., 2023. Genetic study of the American horseshoe crab throughout its Mexican distribution. Conservation and management implications. Biodiversity and Conservation 32, 489–507.

Goodman, A., Anderson, B.M., Allmon, W.D., Crowley, K., Farnsworth, A., Hopkins, M.J., Lunt, D.J., Myers, C., 2025. Global climate model comparisons of niche evolution in turritelline gastropods across the end-cretaceous mass extinction. Paleobio. 51, 452–474.

Hadly, G., 1987. Explanatory notes to the Geological map of the Sahl Al Matran Quadrangle, sheet 26 C, Kingdom of Saudi Arabia. Saudi Arabian Deputy Ministry for Mineral Resources 272, 1–24.

Harper, D.A., Zhan, R.-B., Jin, J., 2015. The Great Ordovician Biodiversification Event: reviewing two decades of research on diversity's big bang illustrated by mainly brachiopod data. Palaeoworld 24, 75–85.

Helal, A.H., 1964. On the occurrence of lower Paleozoic rocks in Tabuk area, Saudi Arabia. Neues Jahr. Geol. Palao. Monat. 7, 391–414.

Helal, A.H., 1968. Stratigraphy of outcropping Paleozoic rocks around the northern edge of the Arabian Shield (within Saudi Arabia). Zeit. Deut. Geol. Gesell. 117, 506–543.

Heymons, R., 1901. Die Entwicklungsgeschichte der Scolopender. Zoologica 13, 1–244.

Kass, J.M., Muscarella, R., Galante, P.J., Bohl, C.L., Pinilla-Buitrago, G.E., Boria, R.A., Soley-Guardia, M., Anderson, R.P., 2021. ENMeval 2.0: Redesigned for customizable and reproducible modeling of species' niches and distributions. MEE 12, 1602–1608.

King, T.L., Eackles, M.S., Aunins, A.W., Brockmann, H.J., Hallerman, E., Brown, B.L., 2015. Conservation genetics of the American Horseshoe Crab (*Limulus polyphemus*): allelic diversity, zones of genetic discontinuity, and regional differentiation, In: Carmichael, R.H., Botton, M.L., Shin, P.K.S., Cheung, S.G. (Eds.), Changing Global Perspectives on Horseshoe Crab Biology, Conservation and Management. Springer International Publishing, Cham, pp. 65–96.

Kocsis, Á.T., Raja, N.B., Williams, S., 2023. rgplates: R interface for the GPlates Web service and desktop application.

Kushlina, V.B., Dronov, A.V., 2011. A giant *Rusophycus* from the Middle Ordovician of Siberia. Ordovician of the World 14, 279–285.

Lamsdell, J.C., 2020. The phylogeny and systematics of Xiphosura. PeerJ 8, e10431.

Lamsdell, J.C., 2025. The first Silurian horseshoe crab reveals details of the xiphosuran ground plan. Proc. R. Soc. B 292, 20250874.

Lamsdell, J.C., Falk, A.R., Hegna, T.A., Meyer, R.C., 2025. Exceptionally preserved ovaries in an ancient horseshoe crab. Geology.

Lamsdell, J.C., Isotalo, P.A., Rudkin, D.M., Martin, M.J., 2023. A new species of the Ordovician horseshoe crab *Lunataspis*. Geol. Mag. 160, 167–171.

Lamsdell, J.C., Ocon, S.B., 2025. Segmentation in early Xiphosura and the evolution of the thoracetron. J. Pal. 1–20.

Latreille, P.A., 1802. Histoire naturelle, générale et particulière, des crustacés et des insectes. Dufart, Paris.

Le Hérissé, A., Vecoli, M., Guidat, C., Not, F., Breuer, P., Wellman, C., Steemans, P., 2017. Middle Ordovician acritarchs and problematic organic-walled microfossils from the Saq-Hanadir transitional beds in the QSIM-801 well, Saudi Arabia. Rev. Micropal. 60, 289–318.

Leibach, W.W., Rose, N., Bader, K., Mohr, L.J., Super, K., Kimmig, J., 2021. Horseshoe crab trace fossils and associated ichnofauna of the Pony Creek Shale Lagerstätte, Upper Pennsylvanian, Kansas, USA. Ichnos 28, 34–45.

Leschen, A.S., Grady, S.P., Valiela, I., 2006. Fecundity and spawning of the Atlantic horseshoe crab, *Limulus polyphemus*, in Pleasant Bay, Cape Cod, Massachusetts, USA. Mar. Ecol. 27, 54–65.

Lomax, D.R., Racay, C.A., 2012. A long mortichnial trackway of *Mesolimulus walchi* from the Upper Jurassic Solnhofen Lithographic Limestone near Wintershof, Germany. Ichnos 19, 175–183.

McClure, H.A., 1978. Early Paleozoic glaciation in Arabia. Palaeogeogr. Palaeoclimatol. Palaeoecol. 25, 315–326.

Quennell, A.M., 1951. The Geology and Mineral Resources of (Former) Trans-Jordan. Colon. Geol. Mineral Resour. 2, 85–115.

Rasul, N.M.A., Stewart, I.C., Nawab, Z.A., 2015. Introduction to the Red Sea: its origin, structure, and environment, The Red Sea: The formation, morphology, oceanography and environment of a young ocean basin. Springer, Berlin, Heidelberg, pp. 1–28.

Romano, M., Whyte, M., 1990. *Selenichnites*, a new name for the ichnogenus *Selenichnus* Romano & Whyte, 1987. Proc. York. Geol. Soc. 48, 221.

R Core Development Team, 2021. R: A language and environment for statistical computing. R Foundation for Statistical Computing, Vienna, Austria.

Romano, M., Whyte, M.A., 1987. A limulid trace fossil from the Scarborough Formation (Jurassic) of Yorkshire; its occurrence, taxonomy and interpretation. Proc. York. Geol. Soc. 46, 85–95.

Romano, M., Whyte, M.A., 2003. The first record of xiphosurid (arthropod) trackways from the Saltwick Formation, Middle Jurassic of the Cleveland Basin, Yorkshire. Palaeontol. 46, 257–269.

Romano, M., Whyte, M.A., 2015. A review of the trace fossil *Selenichnites*. Proc. York. Geol. Soc. 60, 275–288.

Rudkin, D.M., Young, G.A., 2009. Horseshoe crabs–an ancient ancestry revealed. In: Tanacredi, J.T., Botton, M.L., Smith, D.R. (Eds.), Biology and Conservation of Horseshoe Crabs. Springer, New York, pp. 25–44.

Rudkin, D.M., Young, G.A., Nowlan, G.S., 2008. The oldest horseshoe crab: a new xiphosurid from late Ordovician Konservat-Lagerstätten deposits, Manitoba, Canada. Palaeontol. 51, 1–9.

Sagoo, N., Valdes, P., Flecker, R., Gregoire, L.J., 2013. The Early Eocene equable climate problem: can perturbations of climate model parameters identify possible solutions? Phil. Trans. R. Soc. A. 371, 20130123.

Scotese, C.R., 2016. Tutorial: PALEOMAP paleoAtlas for GPlates and the paleoData plotter program. Technical Report, 56. Available at: https://www. earthbyte. org/ paleomap.

Scotese, C.R., Wright, N., 2018. PALEOMAP paleodigital elevation models (PaleoDEMS) for the Phanerozoic. Paleomap Proj.

Servais, T., Harper, D.A.T., 2018. The Great Ordovician Biodiversification Event (GOBE): definition, concept and duration. Lethaia 51, 151–164.

Servais, T., Owen, A.W., Harper, D.A.T., Kröger, B., Munnecke, A., 2010. The Great Ordovician Biodiversification Event (GOBE): the palaeoecological dimension. Palaeogeogr. Palaeoclimatol. Palaeoecol. 294, 99–119.

Shuster Jr., C.N., 1982. A pictorial review of the natural history and ecology of the horseshoe crab *Limulus polyphemus*, with reference to other Limulidae. Prog. Clin. Biol. Res. 81, 1–52.

Shuster Jr., C.N., 2001. Two perspectives: horseshoe crabs during 420 million years, worldwide, and the past 150 years in the Delaware Bay area, In: Tanacredi, J.T. (Ed.), *Limulus* in the Limelight. Springer, New York, pp. 17–40.

Shuster Jr., C.N., Barlow, R.B., Brockmann, H.J., 2003. The American Horseshoe Crab. Harvard University Press, Cambridge.

Siveter, D.J., Selden, P.A., 1987. A new, giant xiphosurid from the lower Namurian of Weardale, County Durham. Proc. York. Geol. Soc. 46, 153–168.

Størmer, L., 1952. Phylogeny and taxonomy of fossil horseshoe crabs. J. Pal. 26, 630–640.

Strother, P.K., Traverse, A., Vecoli, M., 2015. Cryptospores from the Hanadir Shale member of the Qasim Formation, Ordovician (Darriwilian) of Saudi Arabia: taxonomy and systematics. Rev. Palaeobot. Palyn. 212, 97–110.

Sun, Z., Zhao, F., Zeng, H., Erwin, D.H., Zhu, M., 2025. Episodic body size variations of early Paleozoic trilobites associated with marine redox changes. Sci. Av. 11, eadt7572.

Tang, Q., Shingate, P., Wardiatno, Y., John, A., Tay, B.H., Tay, Y.C., Yap, L.M., Lim, J., Tong, H.Y., Tun, K., 2021. The different fates of two Asian horseshoe crab species with different dispersal abilities. Evolut. Appli. 14, 2124–2133.

Valdes, P.J., Armstrong, E., Badger, M.P.S., Bradshaw, C.D., Bragg, F., Crucifix, M., Davies-Barnard, T., Day, J.J., Farnsworth, A., Gordon, C., 2017. The BRIDGE HadCM3 family of climate models: HadCM3@ Bristol v1. 0. Geosci. Model Dev. 10, 3715–3743.

Valdes, P.J., Scotese, C.R., Lunt, D.J., 2021. Deep ocean temperatures through time. Clim. Past 17, 1483–1506.

Van Roy, P., Briggs, D.E.G., Gaines, R.R., 2015. The Fezouata fossils of Morocco; an extraordinary record of marine life in the Early Ordovician. J. Geol. Soc. 172, 541–549.

Vermeij, G.J., 2016. Gigantism and its implications for the history of life. PLoS One 11, e0146092.

Webby, B.D., Paris, F., Droser, M.L., Percival, I.G., 2004. The Great Ordovician Biodiversification Event. Columbia University Press, New York.

Weber, B., Braddy, S.J., 2003. A marginal marine ichnofauna from the Blaiklock Glacier Group (? Lower Ordovician) of the Shackleton Range. Antarctica. Earth Envir. Sci. Trans. Roy. Soc. Edin. 94, 1–20.

Weygoldt, P., Paulus, H.F., 1979. Untersuchungen zur Morphologie, Taxonomie und Phylogenie der Chelicerata. Zeit. Zool. Syst. Evolutionsforschung 17 (85–115), 177–200.

Wickham, H., Chang, W., Wickham, M.H., 2016. Package 'ggplot2'. Create elegant data visualisations using the grammar of graphics. Version 2, 1–189.